Full-scale Atlas motion platform: structure, actuation, and control

Z. Copeland, B. Jung, M.J.D. Hayes* and R.G. Langlois

Department of Mechanical and Aerospace Engineering,
Carleton University,
1125 Colonel By Drive,
Ottawa, ON, K1S 5B6 Canada
Email: Zack.Copeland@carleton.ca
Email: Bradley.Jung@carleton.ca
Email: John.Hayes@carleton.ca
Email: Robert.Langlois@carleton.ca
*Corresponding author

Abstract: This paper presents an overview of the design of the first full-scale prototype of the Atlas flight simulator motion platform for pilot training. The Atlas concept was introduced in 2005, and is unique such that orientation is decoupled from positioning, and unlimited rotations are possible about any axis of the mechanism. Detail design and manufacturing are complete, and assembly is in progress. Central to the design are three Mecanum wheels in an equilateral arrangement, which impart angular displacements to a sphere that houses the cockpit, thereby providing rotational actuation. Since the Atlas sphere rests on these Mecanum wheels, there are no joints or levers constraining its motion, allowing full 360° rotation about all axes, yielding an unbounded orientation workspace that is singularity free. In this paper, the current state of the design and assembly regarding actuation, the spherical S-glass shell, and modelling for motion control are discussed.

Keywords: actuation; simulated dynamic response; structural design; unbounded orientation workspace.

Reference to this paper should be made as follows: Copeland, Z., Jung, B., Hayes, M.J.D. and Langlois, R.G. (2016) 'Full-scale Atlas motion platform: structure, actuation and control', *Int. J. Mechanisms and Robotic Systems*, Vol. 3, Nos. 2/3, pp.94–112.

Biographical notes: Z. Copeland received his BEng (2015) in Mechanical Engineering from Carleton University, Ottawa, ON, Canada. He is working on an MASc in robotic calibration techniques at Carleton. His interests include manufacturing and production technologies, as well as robotics. He enjoys manufacturing and implementation, as well as software design.

B.J. Jung received his BEng (2014) in Aerospace Engineering from Carleton University, Ottawa, ON, Canada. He is working on an MASc in low-cost, reconfigurable flight simulator instruments at Carleton. He is interested in aerodynamics, fluid mechanics, and flight simulation. He enjoys working with electronics, designing software, and implementing dynamic models.

M. John D. Hayes received his BEng (1995), MEng (1996), and PhD (1999) from McGill University in Montreal, QC, Canada. He is currently a Full

Professor in the Department of Mechanical and Aerospace Engineering at Carleton University in Ottawa, ON, Canada. His research interests include computational kinematics, algebraic geometry, and optimisation as they apply to robot mechanical systems design, calibration, and simulation.

Robert G. Langlois received his Engineering Diploma (1987) from St. Francis Xavier University in Antigonish, NS, Canada and BSc (1990), MSc (1991), and PhD (1996) from Queen's University in Kingston, ON, Canada. He is currently a Full Professor in the Department of Mechanical and Aerospace Engineering at Carleton University in Ottawa, ON, Canada. His research interests include applied dynamics, multibody dynamics, and mathematical modelling and simulation as they apply to vehicles and shipboard dynamic systems.

This paper is a revised and expanded version of a paper entitled 'Atlas Motion Platform Full-scale Prototype: Structural Design; Actuation; Motion Control' presented at *3rd Item Symposium on Mechanism Design for Robotics (MEDER)* 2–4 June, 2015, Aalborg, Denmark.

1 Introduction

Conceptually introduced in 2005, the Atlas simulator motion platform is a six degree of freedom (DOF) flight simulator mechanical system that overcomes motion limitations associated with industry-standard simulator motion platforms based on hexapods (Hayes and Langlois, 2005). Unique to the design of Atlas is a three-dimensional translational workspace, which is decoupled from its unbounded, singularity-free orientation workspace. The concept has been incrementally advanced over the last 11 years progressing through a variety of small-scale proof-of-concept prototypes. Assembly of the first full-scale prototype commenced in 2015 (Figure 1). The Atlas concept consists of a cockpit encased in a 9.5 foot diameter composite sphere, which rests on three active Mecanum wheels. The Mecanum wheel is one design for a wheel, which can move a vehicle in any direction. It is sometimes called the Ilon wheel after its Swedish inventor, Bengt Ilon, who came up with the idea in 1973 when he was an engineer with the Swedish company Mecanum AB (Ilon, 1975). Mecanum wheels provide grip in the axial direction of the free-spinning castor rollers mounted to the periphery of the wheel's circumference while allowing passive motion in all other directions. The geometry of the wheels (Gfrerrer, 2008) enables three linear combinations of active wheel angular velocities to spin the sphere about an axis established by the linear combination of wheel speeds. The three Mecanum wheels are strategically spaced around the sphere, arranged on the edges of an equilateral triangle giving an angular separation of 120° in the horizontal plane. The reason for the equilateral configuration is to achieve even force and torque distribution on the Mecanum wheels. The sphere/Mecanum assembly is connected to a 3-DOF translational motion stage. The active Mecanum wheels control the orientation of the sphere, while the linear stage provides for the translation of the platform. This allows for a full 6-DOF motion with unbounded rotation about any axis. Currently, a MOOG MB-EP-6DOF Gough-Stewart platform (Gough, 1956; Stewart, 1965) is used to provide translational actuation.

The Atlas motion platform concept is unique relative to all existing motion platforms, to the best of the authors's knowledge. Hence, there is no literature that can be cited regarding the angular displacement of the sphere using Mecanum wheels. Regardless, the

concept of spherical actuation is not new. Spherical DC induction motors were introduced in 1959 (Williams, Laithwaite, and Eastham, 1959) and developed over the next 30 years, see Chirikjian and Stein (1999); Roth and Lee (1995), for example. However, due to physical limitations imposed by the stator and commutator, angular displacements are limited. Unbounded rotational motion is achieved by the Eclipse II architecture (Kim et al., 2002); however, there is no closed-form algebraic model for its kinematics and the velocity-level kinematics require estimating parameters numerically. The Desdemona motion platform (Bles and Groen, 2009) uses a fully-gimballed system to enable rotation about any axis. However, because of the gimbal arrangement, the orientation workspace is not free of singularities because of the potential of gimbal-lock. There is one other robotic motion platform that could be argued to possess, under certain circumstances, an unbounded orientation workspace, and that is Robocoaster (Schaetzle, Preusche, and Hirzinger, 2009). This is a very clever idea wherein a seat is mounted to the tool flange of a heavy payload six-axis serial robot. However, because the kinematic architecture possesses singular configurations within the reachable workspace, the orientation workspace contains axes about which unbounded rotations are not possible.

Figure 1 A 3D rendering of the Atlas simulator (see online version for colours)

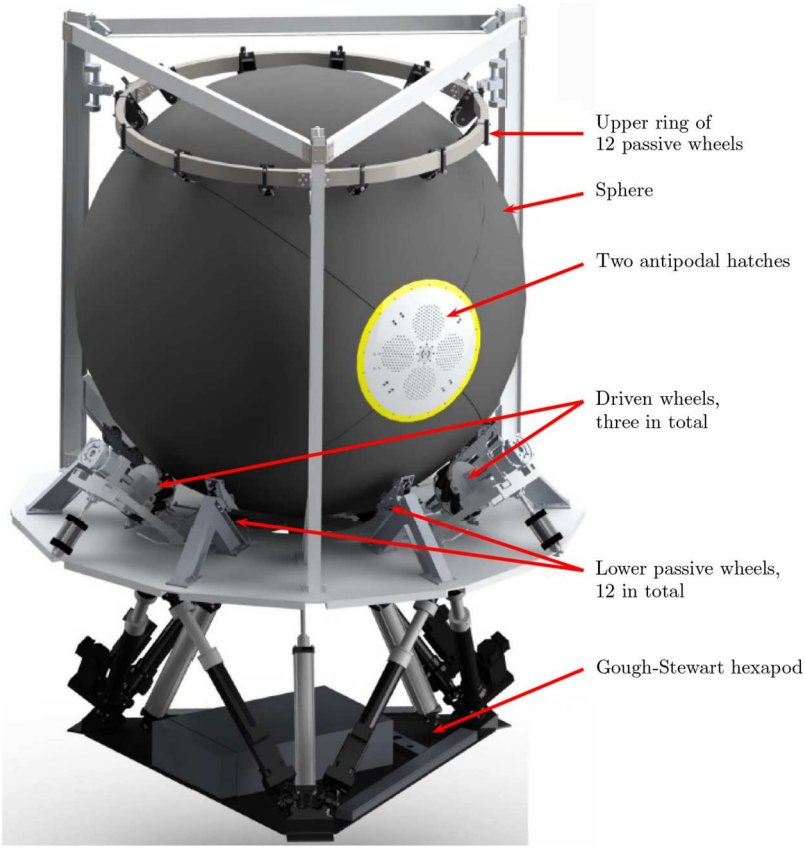

There is a significant body of literature describing various aspects of ground vehicles whose displacement is generated with various types of omni-directional and Mecanum wheels. To the best of the authors's knowledge, the first such paper published was Jonsson

(1985) wherein the author describes the kinematics for automated guided vehicles (AGVs) that use omni-directional wheels for zero turn radius. The first AGV using Mecanum wheels for motion in the plane can be found in Muir and Neuman (1987), which details the kinematic model of a four-Mecanum-wheeled AGV. In Dickerson and Lapin (1991), the authors explore three areas regarding Mecanum-wheeled ground vehicles: the ability to manoeuvre in congested spaces; the kinematics of wheel design; and considerations for wheel loading and traction. Many more publications regarding dynamics, control and optimisation regarding Mecanum and omni-directional-wheeled ground vehicles exist, (see Leow, Low and Loh, 2002; Williams et al. 2002; Salih et al. 2006) for example, but other than Atlas, no literature exists regarding spherical motion generated with Mecanum wheels.

Based on the performance of several proof-of-concept small-scale demonstrators, design of the Atlas full-scale prototype began in 2011 and manufacturing began in earnest in 2013. The assembly of all of the individual components is very near completion. In this paper, the current state of the design and assembly regarding actuation, the spherical S-glass shell, and modelling for motion control are discussed. Please note that the use of Imperial dimensioning reflects the reality of design in Canada: the standard is metric; however, many stock components are sized in Imperial units.

1.1 Motivation

The category of *D-class full-flight simulators* involves the highest standards of fidelity whose motion cues are generated by a motion platform, washed out to return the platform to a kinematically neutral configuration to await the next control input from the trainee, and sustained by the visualisation system. Hexapods are the typical kinematic configuration for the motion platform. While the kinematics are enormously complicated (Husty, 1996), there is significant industrial history and experience. Control systems have matured to become reliable, though still complicated, owing largely to the kinematics.

A typical hexapod can be seen in Figure 1 beneath the Atlas sphere. A significant kinematic limitation to this class of platform is its very limited workspace. Positions and orientations of the cockpit are highly coupled because they are manipulated by changing the lengths of the six prismatic legs. Leg interference further diminishes the reachable workspace. Typically the orienting limits are $\pm 30^\circ, \pm 30^\circ, \pm 50^\circ$ in roll, pitch, and yaw, respectively, (Akdağ, Karagülle, and L Malgaca 2012; Angeles 1997) for example. Actuation is generally achieved with hydraulics or electric ball screws. This is the current industry standard for full-flight simulator motion platforms.

Gawron, Bailey, and Lehman (1995) determined, through studies addressing simulator effectiveness in training, that, based on a range of vehicle types and applications, *high-fidelity* simulation requires roll, pitch, and yaw angular displacement ranges in excess of 180°. These minimums are not achieved by most existing commercial motion bases. Recognising the kinematic and dynamic shortcomings of the industry standard hexapod, the authors strove to identify conceptual motion platform designs that would overcome the hexapod shortcomings regarding angular displacement, and have the appropriate kinematic architecture that would make the platform an appropriate motion base for as broad a range of vehicle types as possible. This has been accomplished by the design of Atlas. It permits unlimited angular displacements about any (every) axis through the geometric centre of the sphere.

2 Structural components

Structural components within the Atlas motion platform can be broken into three main categories for consideration: external structures, the spherical cockpit, and the internal support structures. Due to weight restrictions, a large number of the Atlas components are machined out of 6061 T6 aluminium. Bolt-together designs are employed wherever possible for ease of assembly, maintenance, and future modification.

The primary focus of the external structure of the Atlas prototype is to provide support and stability throughout a wide range of simulated conditions. In order to accomplish this task, it must perform several simultaneous functions: it must allow for the spherical cockpit to be constrained under expected operational loading conditions and provide enough space for the actuation components to be mounted and stabilised.

Support is provided by three vertical I-beams, in an equilateral arrangement, along the outside of the sphere (Figures 1 and 2). The sphere is constrained with two sets of passive Mecanum wheels, connected to the I-beams, located at the top and bottom of the sphere. The 12 passive Mecanum wheels placed along the bottom of the sphere help to distribute its weight and that of the internal structures, while the upper set of 12 passive Mecanum wheels provide downward force to ensure sufficient contact force between the sphere and the three active Mecanum wheels such that the sphere can be rotated. The downward force is supplied by three pneumatic cylinders connected between the I-beams and the upper ring of 12 wheels.

Figure 2 The full-scale Atlas prototype in its present state (see online version for colours)

2.1 Sphere structure

In order to create unbounded rotation, the cockpit of the Atlas prototype is housed in a 9.5 ft diameter fiberglass sphere, consisting of an internal support structure for increased rigidity as well as two hatches to facilitate entry and egress. Due to mechanical and spacial design constraints, the sphere shell is designed so as to be comprised of four identical quarter spheres. Using epoxy and S-glass, the strength required to maintain integrity under the loading from the active Mecanum wheels was achieved. Through consultations with the composites company which was contracted to produce the sphere segments, a failure load in excess of 1000 psi is expected. Although this failure load is an estimation, it was determined experientially alongside the composites company based upon expected resin impregnation characteristics, strength of the fiberglass cloth being used, as well as the shape and loading characteristics of the system as a whole.

Each flange between sphere segments is bound together with a series of bolts, while an aluminium reinforcement is applied to both sides of the joining flanges in order to provide additional stiffness to the sphere, as well as serving as a continuous washer for the bolts to prevent damage to the sphere flanges. In addition to these stiffeners, a series of ribs that serve as a mounting interface for the internal structures is also connected at a 90° angle to the flange stiffeners. Figure 3 illustrates the ribs and stiffeners, as well as how the sphere was assembled; incrementally, one panel at a time.

Figure 3 Assembling the four sphere pannels (see online version for colours)

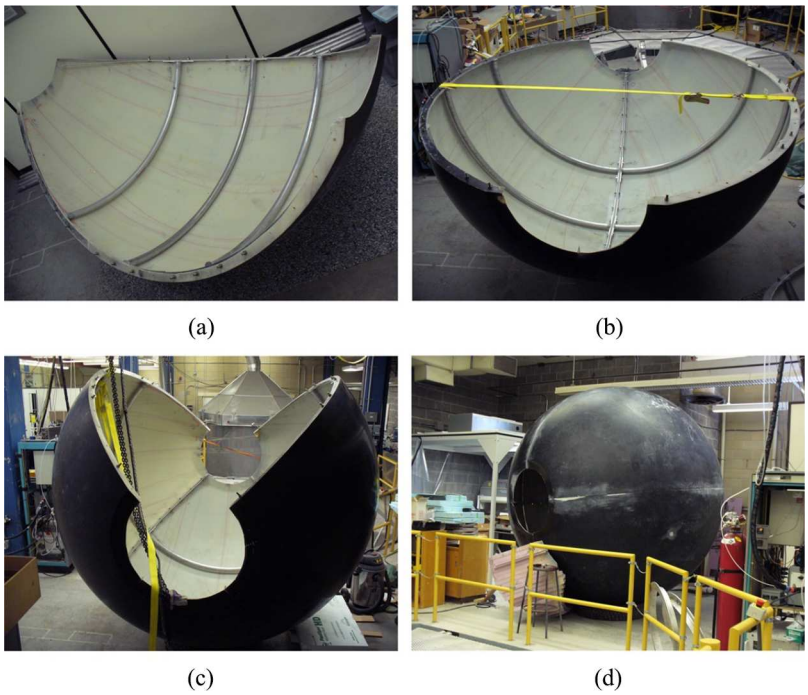

Entry points are included at two antipodal points of the sphere. They comprise two 30 in diameter hatches possessing the same curvature as the sphere. The hatches are locked in place with a striker bolt system, which connects to the internal support structure of the

sphere. The hatches are formed from 3/8 in thick machined aluminium, and are shown in Figure 4. Air circulation is provided to the pilot with four electrically-powered fans placed on each hatch, which make use of 436 contoured ventilation holes in each hatch to allow for each fan to draw and expel air from and to the surroundings.

Figure 4 (a) Top down view of one Atlas hatch; (b) detailed view of contoured ventilation holes (see online version for colours)

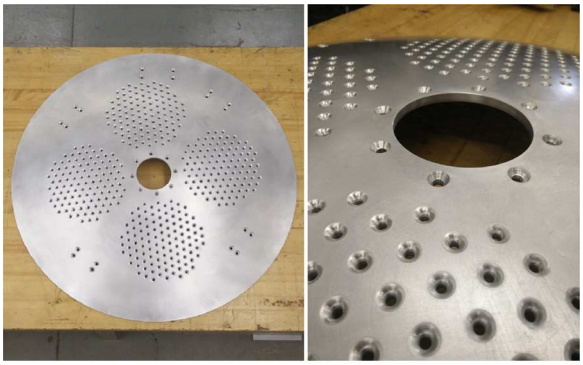

(a) (b)

Attached to the internal support structures are the brackets and flooring that provide a base for the cockpit, seen in Figure 5a. Reconfigurability created the demand for a highly-modular internal structure, so it is bracket and bolt based, allowing for any single component to be reconfigured without requiring disassembly of the sphere. The flooring support structure interfaces with the stiffeners through four brackets, which are bolted to them directly.

Figure 5 (a) Floor structure and pilot support system; (b) interface platform which supports the sphere is attached to the Moog hexapod (see online version for colours)

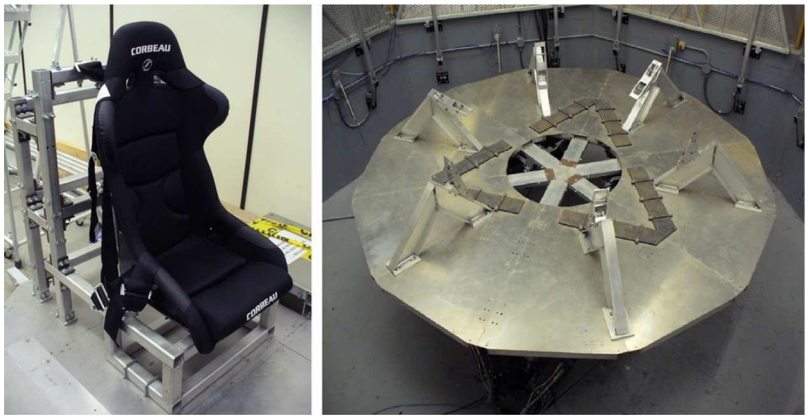

(a) (b)

3 Sphere internal electronics

Unbounded rotation necessitates wireless communication and the use of batteries in order to power the internal electronics of the sphere; LED lighting strips, ventilation fans, environmental sensors, as well as the internal sphere PC. The batteries are removed from the sphere to be recharged after each simulation run. The LED lighting strips are attached to the interior ribs of the sphere, providing illumination for entry, egress, and operation.

While in operation, the interior of the sphere is a closed physical system. This requires that the internal temperature, humidity, CO_2 levels, and power levels be monitored. The sphere PC runs X-Plane 10 flight simulation software, the sensor monitoring system, audio and video feeds, and flight controls. The cockpit consists of a generic central control stick, common to many agile fixed-wing aircraft, throttle and pedals. The pilot also has an emergency stop button in case of an event occurring, which requires the simulator systems to stop.

4 Actuation

The Atlas motion platform possesses six degrees of freedom. What distinguishes Atlas from conventional motion platforms is that linear displacements are decoupled from angular displacements. Moreover, the orientation workspace is unbounded and free from singularities (Klumper et al., 2013). This is accomplished by attaching the sphere orientation system to an interface platform atop a hexapod, see Figure 5b. A MOOG MB-EP-6DOF Gough-Stewart platform was selected to be the hexapod motion base. While this platform is capable of full 6-DOF motion, its controller enables the use of only its translation capabilities Moog (2009), thereby providing linear combinations of surge, sway, and heave. The translation-only motion gives the platform more actuation space in those degrees of freedom due to the fact that high tilt angles restrict actuator stroke lengths, and therefore the overall motion envelope of the platform. With more of the motion envelope accessible at any given time, the simulator is expected to allow smoother washout, thereby increasing motion cueing fidelity.

The orientation degrees of freedom are supplied by the three active Mecanum wheels which supply torque to the sphere, and the 12 pneumatically-controlled upper passive wheels ensure sufficient normal forces at the sphere-active wheel contact patches, while the 12 lower passive Mecanum wheels help support the sphere load. Initially, omniwheels were to provide this rotational actuation, as seen in Figure 6b but Mecanum wheels were ultimately selected in order to reduce actuation-induced vibrations (Weiss, Langlois, and Hayes, 2014). The reduction in vibration is similar to that achieved when helical gear pairs are used in place of corresponding spur gear pairs. Figure 6a is an image of one of the passive Mecanum wheels designed to support the weight of the sphere. While commercial Mecanum wheels exist, appropriate sizing and weights were problematic. Hence, the active wheels were designed in several iterations leading to the final versions illustrated in the figures. The passive Mecanum wheels are substantially smaller than their active counterparts, as illustrated in Figure 7.

Analysis revealed that a normal force of 1500 lbf between each active roller and the sphere is required to enable the active Mecanum wheel rollers to change the sphere orientation without slip in the tractive direction. To ensure an appropriate distribution of this force at each contact point without delamination of the S-glass requires that the forces

be distributed over an area of at least 2.5 in.^{2}, while ensuring that the roller material is stiff enough to avoid deflecting to the point that the hubs would abrade the sphere during operation. Urethane was selected because of favourable wear characteristics and strength limits that are adequate for the expected loading of the Atlas prototype, as well as having a large range of durometers (levels of compliance) to choose from. Testing was conducted in an MTS press, shown in Figure 8a, to establish suitable urethane durometer. Contact patch size was recorded through an ink stamp test where the roller was compressed onto a sheet of paper and analysed photogrammetrically. A sample ink blot can be seen in Figure 8b. This led to the determination of the effective pressure exerted on the sphere surface.

Figure 6 (a) CUSP Mecanum wheel design; (b) omniwheel proof of concept model (see online version for colours)

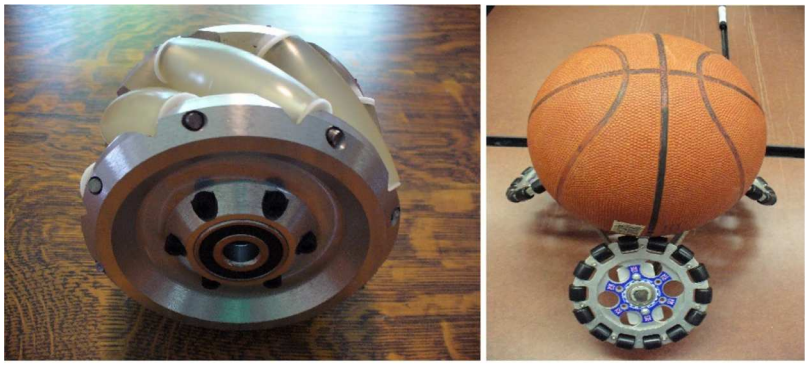

(a) (b)

Figure 7 (a) Atlas active wheel hub; (b) Atlas passive wheel hub assembly (see online version for colours)

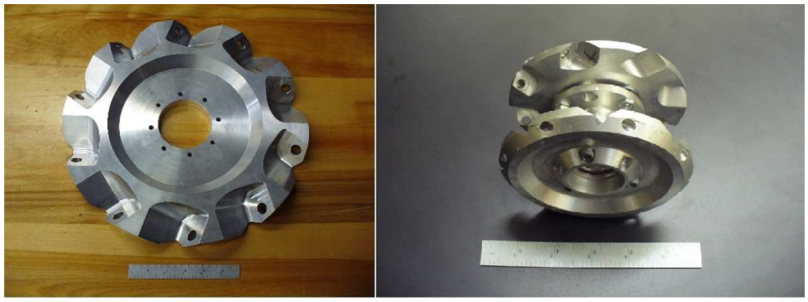

(a) (b)

The analysis revealed that the two durometers of urethane considered for testing, 55A and 85A, both satisfied the minimum required surface contact patch size of 2.5 in.^{2}. While the durometer 55A urethane had surface areas in excess of 5 in.^{2}, it experienced longitudinal deflections on the order 0.5 in., indicating that it would likely jam and abrade the sphere during torque transmission. For this reason, the durometer 85A was selected for the rolling surfaces on both the passive and active Mecanum wheels. Operational force limits on the

sphere S-glass surface mean that the maximum surface pressure is 700 psi. The durometer 85A sample was able to maintain a safety factor of at least 1.5 over the operable pressure range expected.

Figure 8 (a) MTS press test frame with sample roller inserted; (b) resulting ink blot after compression testing a durometer 55A urethane to 1300 lbf (see online version for colours)

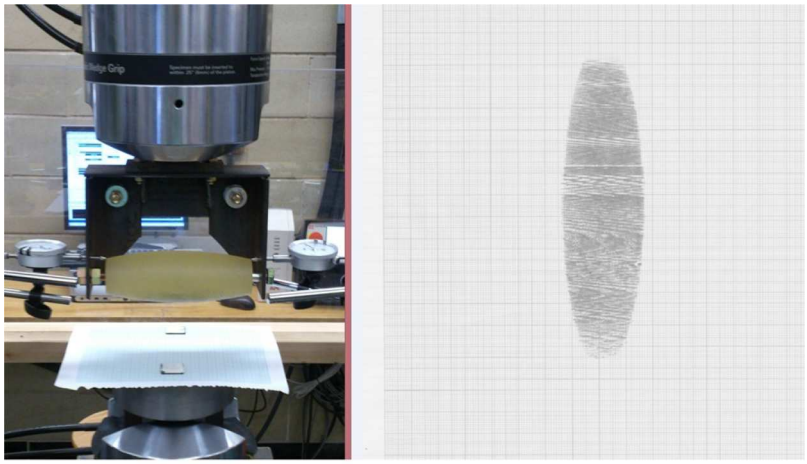

(a) (b)

5 Control, dynamics and simulation

Motion control of the full-scale Atlas platform is based on control algorithms that have been developed and refined incrementally and ultimately prototyped and successfully demonstrated on the half-scale Atlas prototype (Zhou, 2013). Adaptation of the algorithms for use on the full-scale Atlas prototype is supported by a dynamic model to simulate the sphere motions given pilot flight control inputs. The following sections provide a high-level description of the feedback motion control (Klumper et al., 2013), motor torque requirements (Plumpton et al., 2013) and the simulated dynamic response of the sphere.

5.1 Control

The role of the overall Atlas control system is to convert the vehicle state information generated by the on-board vehicle simulation programme into deliberate motions of the Atlas platform such that effective motion cues are provided to the trainee. A central element of the controller is a classical washout filter[1] that has been extended to exploit the large angular motions achievable with Atlas. The washout filter maps simulated vehicle state information to desired translational and rotational motions of the simulator cockpit. The challenge in doing so is to provide effective motion cueing without exceeding the kinematic bounds of the platform. Due to the novel architecture of Atlas, there are no angular displacement limits; however, translational displacement limits as well as both angular and translational limits on velocities and accelerations must be considered. The resulting

coordinated translational and rotational motion commands are sent to the translational stage and rotational stage local controllers, respectively, for the current actuation time step. Translational actuation using the available Stewart-Gough platform actuators is handled by the commercial translational motion platform controller. Control of the rotational stage is achieved using a custom control approach.

Figure 9 provides a high-level block diagram of the rotational stage control architecture. The block labelled *Reference Trajectory* refers to the rotational component of the washout algorithm. The output q_d is the desired platform pose, which is compared with the current measured platform pose q_m, as reported by the orientation-sensing system (OS). The resulting difference between the desired and measured poses e drives a quaternion-based control algorithm that determines the required sphere angular velocity ω_r. Using inverse kinematics that are analogous to the torque Jacobian presented in the following section, the required speeds of the three individual active Mecanum wheels Ω_r can be determined. These are then produced using the individual wheel local motor drive controllers that regulate motor torque to achieve desired speeds. This, in turn, produces the angular motion of the Atlas sphere; which, when combined with the translational motion, creates the desired motion cues for the pilot.

Figure 9 Angular motion feedback control loop

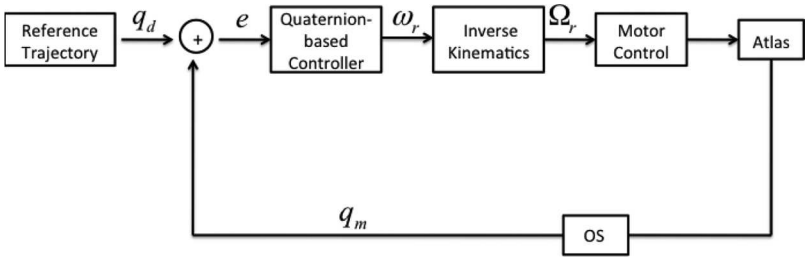

5.2 Sphere orientation sensing

Another challenge in the control system is the determination of the absolute orientation of the rotational stage. For this, a two-part sphere orientation sensing system, which fuses orientation data from a visual orientation system (VOS), that actively tracks circular barcodes affixed to the outer surface of the sphere, and an on-board three-axis gyroscope, is used (Klumper et al., 2013). Figure 10 provides a schematic illustration of how the system functions. The gyroscope provides input data for the inertial orientation sensor system (IOS) at a relatively-high data rate; though it is subject to nondeterministic drift in the determined orientation as time elapses. The camera-based VOS system offers the complementary advantage of being able to measure the absolute orientation of the sphere; though at a much lower data rate than the IOS due to the time required for image processing. Using an Unscented Kalman Filter (UKF) the orientation data can be effectively fused resulting in high-rate, robust and reliable orientation data that is not subject to drift. This system comprises the block labelled *OS* in Figure 9.

Figure 10 Orientation data fusion algorithm

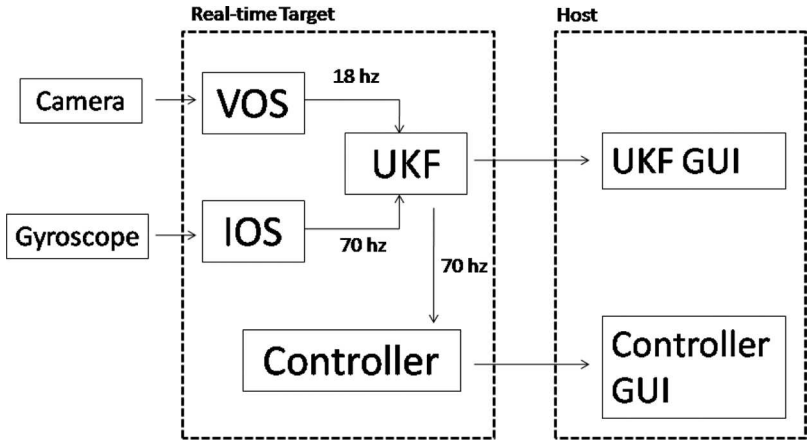

5.3 CUSP simple infrastructure

Each individual simulation subsystem is managed by a federate programme in charge of handling the communication between subsystems and running the necessary control calculations. Core federates directly related to the control of major simulator operations include the ReadVS federate, control federate and washout federate. Vehicle state data is read from the flight simulation software by the ReadVS federate, while the washout federate splits this state data into high- and low-frequency accelerations. The control federate then sends the filtered vehicle state data to the RTP target, which runs the IOS/VOS tracking programme and motor controls. Each federate programme publishes information over the network through UDP where the data may be read by other programmes if they are subscribers.

The CUSP simple infrastructure (CSI) is the custom architecture that binds the various federates together, facilitating the data exchange between the federates on the network, and is illustrated in Figure 11. The network architecture supports both wired and wireless communication such that computing resources located inside the sphere can communicate seamlessly with computing resources located outside the sphere without requiring an umbilical cable for data transfer. The CSI is composed of a dynamically-linked library that is on each machine running a federate programme and the executable that manages data traffic between federates. A proprietary markup language, similar to XML, enables changes to be made to what data is being sent and received. Federates may subscribe in real-time to any other federate.

5.4 Torque Jacobian and simulated dynamic response

The three motors that actuate each of the active Mecanum wheels are positioned equilaterally around the sphere's vertical axis and 45° below the equator, indicated by $\phi = -45°$ for all three wheels, as illustrated in Figure 12a. The Mecanum wheel castor rollers are oriented at a 45° angle relative to the Mecanum wheel axis of rotation, $\gamma = -45°$ for all rollers, as indicated in Figure 12b.

Figure 11 The CUSP simple infrastructure (CSI) (see online version for colours)

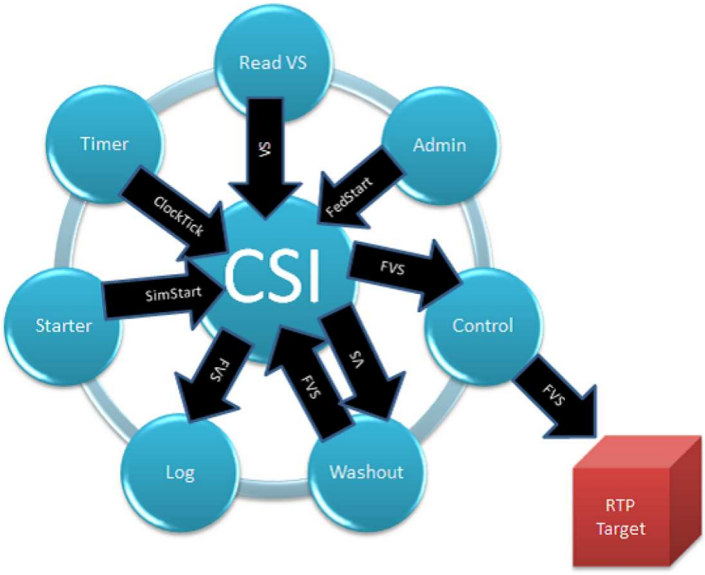

Figure 12 (a) Mecanum wheel position around sphere; (b) roller angles around Mecanum wheel (see online version for colours)

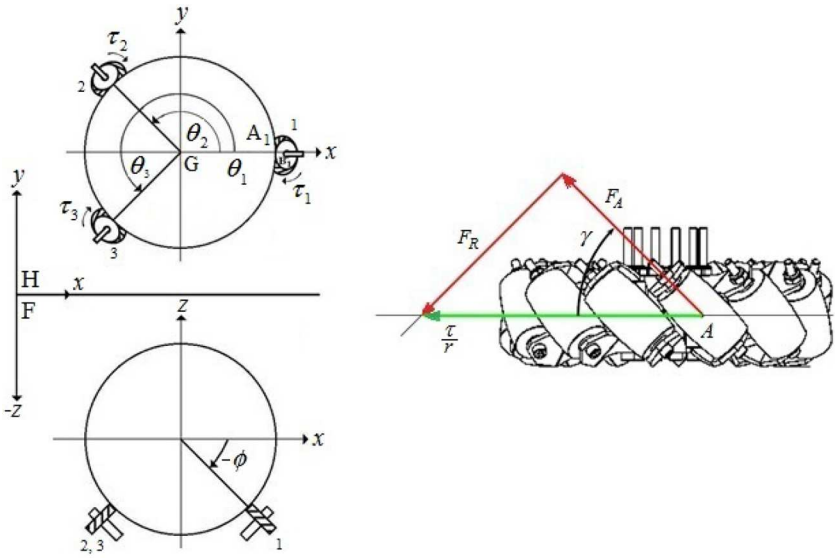

(a) (b)

The total torque $\mathbf{M}$ generated by the Mecanum wheels acting on the sphere is expressed in vector notation as,

$$\mathbf{M} = \left[M_X \; M_Y \; M_Z\right]^T, \tag{1}$$

where the M_i are the torque components expressed in the inertial xyz coordinate system. Position vectors of the idealised Mecanum wheel contact points, A_i, relative to the centre of the sphere G, see Figure 12a, are expressed as:

$$\mathbf{R}_{\mathrm{A_i/G}} = R\left[C\theta_i C\phi_i \; S\theta_i C\phi_i \; S\phi_i\right]^T, \tag{2}$$

where R is the sphere radius, θ_i is the counterclockwise rotation of the $i\mathrm{th}$ wheel, about the Z axis, measured relative to the X axis, while S and C are abbreviations for the sine and cosine functions, respectively. The torque vector generated by each wheel is defined as $\boldsymbol{\tau}_i$, and the Mecanum wheel radial vector points from the $i\mathrm{th}$ wheel centre $\mathrm{B_i}$ to the $i\mathrm{th}$ contact point between castor roller and sphere, $\mathrm{A_i}$:

$$\mathbf{r}_{\mathrm{A_i/B_i}} = r\left[-C\theta_i C\phi_i \; -S\theta_i C\phi_i \; -S\phi_i\right]^T, \tag{3}$$

where r is the radius of the Mecanum wheel. This radial vector possesses the same line of action as $\mathbf{R}_{\mathrm{A_i/G}}$, but in the opposite sense. The Mecanum wheels have tractive force vectors along the roller axes that are given by,

$$\mathbf{F}_{\mathrm{A_i}} = F_{\mathrm{A_i}}\left[-C\theta_i S\gamma_i S\phi_i - S\theta_i C\gamma_i \; -S\theta_i S\gamma_i S\phi_i + C\theta_i C\gamma_i \; S\gamma_i C\phi_i\right]^T, \tag{4}$$

where γ_i is the angle of the Mecanum wheel roller axis relative to the plane of the wheel, and,

$$F_{\mathrm{A_i}} = \frac{\tau_i}{rC\gamma_i}, \tag{5}$$

as illustrated in Figure 12a.

The torque vector, $\mathbf{M}$, generated by the $i\mathrm{th}$ Mecanum wheel acting on the sphere is computed as the cross product of the position vector of the centre of the wheel's contact patch relative to the sphere centre with the force injected to the sphere by the wheel, resulting in the equation,

$$\mathbf{M}_i = \mathbf{R}_{\mathrm{A_i/G}} \times \mathbf{F}_{\mathrm{A_i}} = \frac{\tau_i R}{rC\gamma_i}\left[-C\theta_i C\gamma_i S\phi_i + S\theta_i S\gamma_i, \;\; -S\theta_i C\gamma_i S\phi_i - C\theta_i S\gamma_i, \;\; C\gamma_i C\phi_i\right]^T$$

where the position of the contact patch around the sphere is specified by angle, θ_i, and inclination angle, ϕ_i; the angle the roller axis makes with the Mecanum wheel axis is γ_i; the radius of the sphere is R, the effective radius of the Mecanum wheel is r; the individual Mecanum wheel torques are τ_i. Summing the three sphere torque vectors together results in the total torque applied to the sphere,

$$\mathbf{M} = \sum \mathbf{M}_i = \mathbf{M}_1 + \mathbf{M}_2 + \mathbf{M}_3, \tag{6}$$

such that,

$$\mathbf{M} = \frac{R}{r}\begin{bmatrix} -C\theta_1 S\phi_1 + S\theta_1 T\gamma_1 & -C\theta_2 S\phi_2 + S\theta_2 T\gamma_2 & -C\theta_3 S\phi_3 + S\theta_3 T\gamma_3 \\ -S\theta_1 S\phi_1 - C\theta_1 T\gamma_1 & -S\theta_2 S\phi_2 - C\theta_2 T\gamma_2 & -S\theta_3 S\phi_3 - C\theta_3 T\gamma_3 \\ C\phi_1 & C\phi_2 & C\phi_3 \end{bmatrix} \bar{\boldsymbol{\tau}}, \tag{7}$$

where $\bar{\boldsymbol{\tau}}$ represents the magnitudes of the three Mecanum wheel torques, and T is the abbreviation for tangent. This expression defines the Jacobian $\mathbf{J}_\tau$ between driven wheel torque and sphere actuation torque,

$$\mathbf{M} = \mathbf{J}_\tau \bar{\boldsymbol{\tau}}. \tag{8}$$

Hence, $\mathbf{J}_\tau$ is the torque Jacobian given by,

$$\mathbf{J}_\tau = \frac{R}{r}\begin{bmatrix} -C\theta_1 S\phi_1 + S\theta_1 T\gamma_1 & -C\theta_2 S\phi_2 + S\theta_2 T\gamma_2 & -C\theta_3 S\phi_3 + S\theta_2 T\gamma_3 \\ -C\theta_1 S\phi_1 - S\theta_1 T\gamma_1 & -C\theta_2 S\phi_2 - S\theta_2 T\gamma_2 & -C\theta_3 S\phi_3 - S\theta_2 T\gamma_3 \\ C\phi_1 & C\phi_2 & C\phi_3 \end{bmatrix}. \tag{9}$$

The remarkable thing to note is that the Jacobian is a time-invariant matrix of constant values determined by constant design angles, namely the angular separation between Mecanum wheels, the inclination angle below the horizon of the active wheels and the angle the castor roller axes make with respect to the active Mecanum wheel axes. Hence, the design angles may be selected such that the Jacobian is free from singularities. This in turn means that the orientation workspace is an unbounded, fully-dexterous space (Kumar and Waldron, 1981). This means that at every point within the reachable workspace of the MOOG platform that the sphere can have any desired orientation. Full details regarding the derivation of the Jacobian can be found in Plumpton et al. (2013).

A sphere emulator programme was designed for the purposes of dry testing sphere reactions to motor torques, as well as recording the simulation run for subsequent playback and data analysis, and is illustrated in the screen capture in Figure 13. The emulator reads the desired Mecanum wheel torque data in real time from the custom Atlas simulation computer network or from a previously-saved file and calculates the incremental orientation of the Atlas sphere. The programme takes the sphere's inertial matrix and torque Jacobian matrix into account to provide a dynamic model of the sphere movement. The emulator programme was written in MATLAB and includes a graphical user interface displaying the sphere animation, data readouts and user controls.

Rotation sequences are expressed in the emulator using quaternions to avoid the potential representational singularities presented by rotation matrices. Moreover, a rotation expressed as a quaternion rotation does not rely on a hierarchy of rotations. Quaternions form a four-dimensional associative normed division algebra over the real numbers. A quaternion represents the orientation of a coordinate system attached to a rigid body as a point on the surface of a sphere in a three-dimensional projective space. The quaternion can be interpreted as a single rotation about a specific single axis. Once the desired motion is converted into quaternion notation, the sphere will rotate in a single sweeping motion. This makes motion interpolation between large angle rotations possible. Quaternion algebra and use as a rotation operator is found in many texts, see Diebel (2006); Kuipers (1999) for example. The quaternion can be expressed as:

$$q = q_0 + \mathbf{i}q_1 + \mathbf{j}q_2 + \mathbf{k}q_3. \tag{10}$$

It comprises a scalar part, q_0, and a vector part, q_1, q_2, and q_3:

$$\begin{aligned} q_0 &= cos\,(\alpha/2)\,; \\ q_1 &= sin\,(\alpha/2)\,cos\,(\beta_x)\,; \\ q_2 &= sin\,(\alpha/2)\,cos\,(\beta_y)\,; \\ q_3 &= sin\,(\alpha/2)\,cos\,(\beta_z)\,; \end{aligned} \tag{11}$$

where α is the rotation angle and the β_i are the direction cosines of the rotation axis. Changes in orientation require quaternion products between the initial and final orientations. A quaternion product has the form

$$q \cdot p = \overline{Q}\,(p) \cdot q, \tag{12}$$

where

$$\overline{Q}\,(p) = \begin{bmatrix} q_0 & -q_1 & -q_2 & -q_3 \\ q_1 & q_0 & -q_3 & q_2 \\ q_2 & q_3 & q_0 & -q_1 \\ q_3 & -q_2 & q_1 & q_0 \end{bmatrix}. \tag{13}$$

The moment of inertia matrix, **I**, necessary for dynamic modelling was extracted from the Atlas composite CAD model by estimating the approximate densities of each component in the assembly. This is a 3×3 symmetric matrix that is variable to accommodate changes to the sphere weight distribution between simulation runs. For each simulation cycle, the initial motor torque, angular rate, and sphere attitude (τ, ω_0, ϕ_0) are read by the emulator and then converted to quaternions, which are denoted e_0.

Figure 13 The Atlas emulator user interface (see online version for colours)

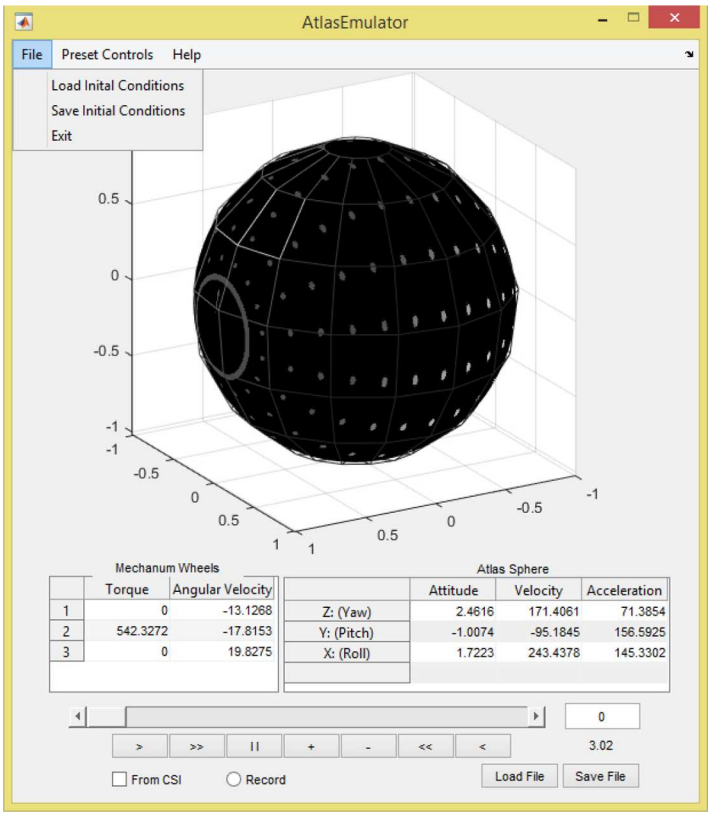

The angular momentum equation can be rearranged as:

$$\boldsymbol{\alpha}_1 = \mathbf{I}^{-1}\left(\mathbf{M} - \boldsymbol{\omega}_0 \times \mathbf{I}\omega_0\right), \tag{14}$$

where $\boldsymbol{\alpha}$ is the sphere angular acceleration. The angular acceleration is numerically integrated resulting in an updated angular velocity:

$$\boldsymbol{\omega}_1 = \boldsymbol{\omega}_0 + \int \boldsymbol{\alpha}_1 \mathrm{d}t. \tag{15}$$

The Euler angle rates are converted to quaternion rates yielding (Diebel, 2006)

$$\dot{e}_1 = \frac{1}{2} L\omega_1, \tag{16}$$

where

$$L = \begin{bmatrix} -q_1 & q_0 & -q_3 & q_2 \\ -q_2 & q_3 & q_0 & -q_1 \\ -q_3 & -q_2 & q_1 & -q_0 \end{bmatrix}. \tag{17}$$

The quaternion rate is then numerically integrated to obtain an updated orientation:

$$e_1 = e_0 + \int \dot{e}_1 \mathrm{d}t. \tag{18}$$

Finally, the quaternion rate is converted back into Euler angle rates. The calculated angular rate and angle are then fed back into the system for the next iteration, $e_1 \rightarrow \phi_1$. This process is then repeated for the duration of the dynamic simulation.

6 Concluding remarks

This paper has presented an overview of the current state of development of the Atlas simulator motion base with emphasis on the rotational actuation system, as well as computational tools that have been developed to support the design and operation of the system. As is apparent from the design, the unusual actuation method provides unique motion capabilities for the simulator: most notably unbounded, singularity-free rotation. However, with that come some practical challenges relating to the need for tether-free power, data transfer and ventilation. As described, these issues were resolved early in the overall simulator design cycle such that their solutions could be incorporated into the detailed design of Atlas. A power-conscious electrical design has allowed the sphere internal systems to be run from a rechargeable battery power source located inside the sphere. Data transfer is enabled using a wireless protocol for communicating the vehicle state information and various sensor measurements out of the sphere as well as various simulation control signals into the sphere. Running the main vehicle simulation on the sphere PC (located inside the sphere) precludes the need for transmitting bandwidth-intensive simulation audio and video streams over the wireless network. Ventilation is provided using forced convection through the sphere generated by eight hatch-mounted fans. In addition, since the drive system is unconventional and relies on technologies for which exact closed-form solutions do not exist in many cases, and despite the fact that the basic design principles are low risk, it is anticipated that much will be learned through the commissioning and calibration phases of the full-scale prototype.

Three related areas of particular interest will be the contact forces, Mecanum wheel tractive forces and wheel slip. In total, the sphere is held in place by patch contact with 27 Mecanum wheels. The system is clearly statically indeterminate and time-varying due to the inertial loads acting on the system as the simulator is in motion and also due to the time-varying tractive forces applied by the active Mecanum wheels. Design tools that were developed to approximate the worst-case contact forces necessarily made assumptions such as: the relative rigidity of the external supporting structure; the effective stiffnesses of both the small and large Mecanum wheel castor assemblies; and the characteristics of urethane in this application. The maximum tractive effort of the active Mecanum wheels will depend both on the prevailing contact forces and the friction characteristics at the interface between the active Mecanum wheels and sphere surface. Initial testing was performed to determine the required durometer of urethane and its friction properties; however, some notable differences between test conditions and in situ operation are anticipated. Finally, wheel slip due to tangential compression of the urethane material prior to it entering the active Mecanum wheel contact patches is expected to result in longitudinal slip, similar to what occurs with pneumatic tires. The extent of this and its impact on the idealised kinematic equations, based upon which the system has been designed, will have to be assessed and integrated into the Atlas control system.

As a result of its unique design, the Atlas simulator, as described in this paper, introduces a significant technical innovation in the ability to generate large angular motions with a simulator motion base. It also presents numerous opportunities for further research and development by the authors and the broader research community.

References

Akdağ, M., Karagülle, H. and Malgaca, L. (2012) 'An integrated approach for simulation of mechatronic systems applied to a hexapod robot', *Mathematics and Computers in Simulation*, Vol. 82, No. 5, pp.818–835.

Angeles, J. (1997) *Fundamentals of Robotic Mechanical Systems: Theory, Methods, and Algorithms*, Springer-Verlag, New York, NY.

Bles, W. and Groen, E. (2009) 'The DESDEMONA motion facility: applications for space research', *Microgravity Science and Technology*, Vol. 21, No. 4, pp.281–286.

Chirikjian, G.S. and Stein, D. (1999) 'Kinematic design and commutation of a spherical stepper motor', *IEEE/ASME Transactions on Mechatronics*, Vol. 4, No. 4, pp.342–353.

Dickerson, S.L. and Lapin, B.D. (1991) 'Control of an Omni-directional robotic vehicle with Mecanum wheels', *Computer Aided Geometric Design*, Vol. 25, No. 9, pp.784–791.

Diebel, J. (2006) *Representing Attitude: Euler Angles, Unit Quaternions, and Rotation Vectors*, *Stanford University*, Stanford, California, U.S.A., October.

Gawron, V.J., Bailey, R. and Lehman, E. (1995) 'Lessons learned in applying simulators to crewstation evaluation', *International Journal of Aviation Psychology*, Vol. 5, No. 2, pp.277–290.

Gfrerrer, A. (2008) 'Geometry and kinematics of the Mecanum wheel', *Computer Aided Geometric Design*, Vol. 25, No. 9, pp.784–791.

Gough, V.E. (1956) 'Discussion in London: automobile stability, control, and tyre performance', *Proc. Automobile Division, Institution of Mech. Engrs.*, pp.392–394.

Hayes, M.J.D. and Langlois, R.G. (2005) 'Atlas: a novel kinematic architecture for six DOF motion platforms', *Transaction of the Canadian Society for Mechanical Engineering*, Vol. 29, No. 4, pp.701–709.

Husty, M.L. (1996) 'An algorithm for solving the direct kinematics of general Stewart-Gough platforms', *Mechanism and Machine Theory*, Vol. 31, No. 4, pp.365–379.

Ilon, B.E. (1975) *Control of an Omni-Directional Robotic Vehicle with Mecanum Wheels*, *US Patent 3876255*, April.

Jonsson, S. (1985) 'New AGV with revolutionary movement', in S.E. Anderson (Ed.): *Proc. 3rd Int. Conf. on Automated Guided Vehicles*, Stockholm, pp.135–144.

Kim, J., Hwang, J-C., Kim, J-S., Iurascu, C.C., Park, F.C. and Cho, Y.M. (2002) 'Eclipse-11: a new parallel mechanism enabling continuous 360-degree spinning plus three-axis translational motions', *IEEE Transactions on Robotics and Automation*, Vol. 18, No. 3, pp.367–373.

Klumper, K., Morbi, A., Chisholm, K.J., Beranek, R., Ahmadi, M. and Langlois, R.G. (2013) *Orientation Control of Atlas: A Novel Motion Simulation Platform*, *No. 13-CSME-192, E.I.C. Accession 3650*, September.

Kuipers, J.B. (1999) *Quaternions and Rotation Sequences*, Princeton University Press, Princeton, NJ.

Kumar, A.V. and Waldron, K.J. (1981) 'The workspace of a mechanical manipulator', *ASME Journal of Mechanical Design*, Vol. 103, No. 3, pp.665–672.

Leow, Y.P., Low, K.H. and Loh, W.K. (2002) 'Kinematic modelling and analysis of mobile robots with omni-directional wheels', *Seventh International Conference on Control, Automation, Robotics and Vision (ICARCV'02),* Singapore, December, pp.820–825.

Moog Inc (2009) *Moog Motion Systems Overview*, Rev 3.11.09.

Muir, P.F. and Neuman, C.P. (1987) 'Kinematic modeling for feedback control of an omni-direction wheeled mobile robot', *IEEE Intenational Conference on Robotics and Automation*, Vol. 25, No. 9, pp.784–791.

Plumpton, J.J., Hayes, M.J.D., Langlois, R.G. and Burlton, B.V. (2013) *Atlas Motion Platform Mecanum Wheel Jacobian in the Velocity and Static Force Domains*, No. 13-CSME-192, E.I.C. Accession 3650, September.

Roth, R.B. and Lee, K-M. (1995) 'Design optimization of a three-degree-of-freedom variable reluctance spherical wrist motor', *ASME Journal of Engineering for Industry*, Vol. 117, pp.378–388.

Salih, J.E.M., Rizon, M., Yaacob, S., Adom, A.H. and Mamat, M.R. (2006) 'Designing omni-directional mobile robot with Mecanum wheel', *American Journal of Applied Sciences*, Vol. 3, No. 5, pp.1831–1835.

Schaetzle, S., Preusche, C. and Hirzinger, G. (2009) 'Workspace optimization of the robocoaster used as a motion simulator', *Proceedings of the 14th IASTED International Conference on Robotics and Applications*, Vol. 1, pp.470–477.

Stewart, D. (1965) 'A platform with six degrees of freedom', *Proceedings of the Institution of Mechanical Engineers*, Vol. 180, No. 15, pp.371–378.

Weiss, A., Langlois, R.G. and Hayes, M.J.D. (2014) 'Dynamics and vibration analysis of the interface between a non-rigid sphere and omnidirectional wheel actuators', *Robotica*, Vol. 33, May, pp.1850–1868.

Williams, R., Carter, D., Gallina, P. and Rosati, G. (2002) 'Dynamics model with slip for wheeled omni-directional robots', *IEEE Transactions on Robotic and Automation*, Vol. 18, No. 3, pp.285–293.

Williams, F., Laithwaite, E.R. and Eastham, G.F. (1959) 'Development and design of spherical induction motors', *Proceedings of IEEE*, Vol. 47, pp.471–484.

Zhou, S. (2013) *Sensing and Vision-Based Control of a Spherical Motion Platform*, M.A.Sc. Thesis, Carleton University, Ottawa, Canada, January.

Note

[1]Washout filter is alternatively referred to as a tilt-coordination algorithm.